CHAPTER ONE

Introduction

1.1 GENERAL

1.1.1 HISTORICAL BACKGROUND

The development of modern computational fluid dynamics (CFD) began with the advent of the digital computer in the early 1950s. Finite difference methods (FDM) and finite element methods (FEM), which are the basic tools used in the solution of partial differential equations in general and CFD in particular, have different origins. In 1910, at the Royal Society of London, Richardson presented a paper on the first FDM solution for the stress analysis of a masonry dam. In contrast, the first FEM work was published in the *Aeronautical Science Journal* by Turner, Clough, Martin, and Topp for applications to aircraft stress analysis in 1956. Since then, both methods have been developed extensively in fluid dynamics, heat transfer, and related areas.

Earlier applications of FDM in CFD include Courant, Friedrichs, and Lewy [1928], Evans and Harlow [1957], Godunov [1959], Lax and Wendroff [1960], MacCormack [1969], Briley and McDonald [1973], van Leer [1974], Beam and Warming [1978], Harten [1978, 1983], Roe [1981, 1984], Jameson [1982], among many others. The literature on FDM in CFD is adequately documented in many text books such as Roache [1972, 1999], Patankar [1980], Peyret and Taylor [1983], Anderson, Tannehill, and Pletcher [1984, 1997], Hoffman [1989], Hirsch [1988, 1990], Fletcher [1988], Anderson [1995], and Ferziger and Peric [1999], among others.

Earlier applications of FEM in CFD include Zienkiewicz and Cheung [1965], Oden [1972, 1988], Chung [1978], Hughes et al. [1982], Baker [1983], Zienkiewicz and Taylor [1991], Carey and Oden [1986], Pironneau [1989], Pepper and Heinrich [1992]. Other contributions of FEM in CFD for the past two decades include generalized Petrov-Galerkin methods [Heinrich et al., 1977; Hughes, Franca, and Mallett, 1986; Johnson, 1987], Taylor-Galerkin methods [Donea, 1984; Löhner, Morgan, and Zienkiewicz, 1985], adaptive methods [Oden et al., 1989], characteristic Galerkin methods [Zienkiewicz et al., 1995], discontinuous Galerkin methods [Oden, Babuska, and Baumann, 1998], and incompressible flows [Gresho and Sani, 1999], among others.

There is a growing evidence of benefits accruing from the combined knowledge of both FDM and FEM. Finite volume methods (FVM), because of their simple data structure, have become increasingly popular in recent years, their formulations being

related to both FDM and FEM. The flowfield-dependent variation (FDV) methods [Chung, 1999] also point to close relationships between FDM and FEM. Therefore, in this book we are seeking to recognize such views and to pursue the advantage of studying FDM and FEM together on an equal footing.

Historically, FDMs have dominated the CFD community. Simplicity in formulations and computations contributed to this trend. FEMs, on the other hand, are known to be more complicated in formulations and more time-consuming in computations. However, this is no longer the case in many of the recent developments in FEM applications. Many examples of superior performance of FEM have been demonstrated. Our ultimate goal is to be aware of all advantages and disadvantages of all available methods so that if and when supercomputers grow manyfold in speed and memory storage, this knowledge will be an asset in determining the computational scheme capable of rendering the most accurate results, and not be limited by computer capacity. In the meantime, one may always be able to adjust his or her needs in choosing between suitable computational schemes and available computing resources. It is toward this flexibility and desire that this text is geared.

1.1.2 ORGANIZATION OF TEXT

This book covers the basic concepts, procedures, and applications of computational methods in fluids and heat transfer, known as computational fluid dynamics (CFD). Specifically, the fundamentals of finite difference methods (FDM) and finite element methods (FEM) are included in Parts Two and Three, respectively. Finite volume methods (FVM) are placed under both FDM and FEM as appropriate. This is because FVM can be formulated using either FDM or FEM. Grid generation, adaptive methods, and computational techniques are covered in Part Four. Applications to various physical problems in fluids and heat transfer are included in Part Five.

The unique feature of this volume, which is addressed to the beginner and the practitioner alike, is an equal emphasis of these two major computational methods, FDM and FEM. Such a view stems from the fact that, in many cases, one method appears to thrive on merits of other methods. For example, some of the recent developments in finite elements are based on the Taylor series expansion of conservation variables advanced earlier in finite difference methods. On the other hand, unstructured grids and the implementation of Neumann boundary conditions so well adapted in finite elements are utilized in finite differences through finite volume methods. Either finite differences or finite elements are used in finite volume methods in which in some cases better accuracy and efficiency can be achieved. The classical spectral methods may be formulated in terms of FDM or they can be combined into finite elements to generate spectral element methods (SEM), the process of which demonstrates usefulness in direct numerical simulation for turbulent flows. With access to these methods, readers are given the direction that will enable them to achieve accuracy and efficiency from their own judgments and decisions, depending upon specific individual needs. This volume addresses the importance and significance of the in-depth knowledge of both FDM and FEM toward an ultimate unification of computational fluid dynamics strategies in general. A thorough study of all available methods without bias will lead to this goal.

Preliminaries begin in Chapter 1 with an introduction of the basic concepts of all CFD methods (FDM, FEM, and FVM). These concepts are applied to solve simple

one-dimensional problems. It is shown that all methods lead to identical results. In this process, it is intended that the beginner can follow every step of the solution with simple hand calculations. Being aware that the basic principles are straightforward, the reader may be adequately prepared and encouraged to explore further developments in the rest of the book for more complicated problems.

Chapter 2 examines the governing equations with boundary and initial conditions which are encountered in general. Specific forms of governing equations and boundary and initial conditions for various fluid dynamics problems will be discussed later in appropriate chapters.

Part Two covers FDM, beginning with Chapter 3 for derivations of finite difference equations. Simple methods are followed by general methods for higher order derivatives and other special cases.

Finite difference schemes and solution methods for elliptic, parabolic, and hyperbolic equations, and the Burgers' equation are discussed in Chapter 4. Most of the basic finite difference strategies are covered through simple applications.

Chapter 5 presents finite difference solutions of incompressible flows. Artificial compressibility methods (ACM), SIMPLE, PISO, MAC, vortex methods, and coordinate transformations for arbitrary geometries are elaborated in this chapter.

In Chapter 6, various solution schemes for compressible flows are presented. Potential equations, Euler equations, and the Navier-Stokes system of equations are included. Central schemes, first order and second order upwind schemes, the total variation diminishing (TVD) methods, preconditioning process for all speed flows, and the flowfield-dependent variation (FDV) methods are discussed in this chapter.

Finite volume methods (FVM) using finite difference schemes are presented in Chapter 7. Node-centered and cell-centered schemes are elaborated, and applications using FDV methods are also included.

Part Three begins with Chapter 8, in which basic concepts for the finite element theory are reviewed, including the definitions of errors as used in the finite element analysis. Chapter 9 provides discussion of finite element interpolation functions.

Applications to linear and nonlinear problems are presented in Chapter 10 and Chapter 11, respectively. Standard Galerkin methods (SGM), generalized Galerkin methods (GGM), Taylor-Galerkin methods (TGM), and generalized Petrov-Galerkin (GPG) methods are discussed in these chapters.

Finite element formulations for incompressible and compressible flows are treated in Chapter 12 and Chapter 13, respectively. Although there are considerable differences between FDM and FEM in dealing with incompressible and compresible flows, it is shown that the new concept of flowfield-dependent variation (FDV) methods is capable of relating both FDM and FEM closely together.

In Chapter 14, we discuss computational methods other than the Galerkin methods. Spectral element methods (SEM), least squares methods (LSM), and finite point methods (FPM, also known as meshless methods or element-free Galerkin), are presented in this chapter. Chapter 15 discusses finite volume methods with finite elements used as a basic structure.

Finally, the overall comparison between FDM and FEM is presented in Chapter 16, wherein analogies and differences between the two methods are detailed. Furthermore, a general formulation of CFD schemes by means of the flowfield-dependent variation (FDV) algorithm is shown to lead to most all existing computational schemes in FDM

and FEM as special cases. Brief descriptions of available methods other than FDM, FEM, and FVM such as boundary element methods (BEM), particle-in-cell (PIC) methods, Monte Carlo methods (MCM) are also given in this chapter.

Part Four begins with structured grid generation in Chapter 17, followed by unstructured grid generation in Chapter 18. Subsequently, adaptive methods with structured grids and unstructured grids are treated in Chapter 19. Various computing techniques, including domain decomposition, multigrid methods, and parallel processing, are given in Chapter 20.

Applications of numerical schemes suitable for various physical phenomena are discussed in Part Five (Chapters 21 through 27). They include turbulence, chemically reacting flows and combustion, acoustics, combined mode radiative heat transfer, multiphase flows, electromagnetic flows, and relativistic astrophysical flows.

1.2 ONE-DIMENSIONAL COMPUTATIONS BY FINITE DIFFERENCE METHODS

In this and the following sections of this chapter, the beginner is invited to examine the simplest version of the introduction of FDM, FEM, FVM via FDM, and FVM via FEM, with hands-on exercise problems. Hopefully, this will be a sufficient motivation to continue with the rest of this book.

In finite difference methods (FDM), derivatives in the governing equations are written in finite difference forms. To illustrate, let us consider the second-order, one-dimensional linear differential equation,

$$\frac{d^2u}{dx^2} - 2 = 0 \quad 0 < x < 1 \tag{1.2.1a}$$

with the Dirichlet boundary conditions (values of the variable u specified at the boundaries),

$$\begin{cases} u = 0 & \text{at } x = 0 \\ u = 0 & \text{at } x = 1 \end{cases} \tag{1.2.1b}$$

for which the exact solution is $u = x^2 - x$.

It should be noted that a simple differential equation in one-dimensional space with simple boundary conditions such as in this case possesses a smooth analytical solution. Then, all numerical methods (FDM, FEM, and FVM) will lead to the exact solution even with a coarse mesh. We shall examine that this is true for this example problem.

The finite difference equations for du/dx and d^2u/dx^2 are written as (Figure 1.2.1)

$$\left(\frac{du}{dx}\right)_i \approx \frac{u_{i+1} - u_i}{\Delta x} \quad \textit{forward difference} \tag{1.2.2a}$$

$$\left(\frac{du}{dx}\right)_i \approx \frac{u_i - u_{i-1}}{\Delta x} \quad \textit{backward difference} \tag{1.2.2b}$$

$$\left(\frac{du}{dx}\right)_i \approx \frac{u_{i+1} - u_{i-1}}{2\Delta x} \quad \textit{central difference} \tag{1.2.2c}$$

$$\frac{d^2u}{dx^2} = \frac{d}{dx}\left(\frac{du}{dx}\right) \cong \frac{1}{\Delta x}\left[\left(\frac{du}{dx}\right)_{i+1} - \left(\frac{du}{dx}\right)_i\right] = \frac{1}{\Delta x}\left(\frac{u_{i+1} - u_i}{\Delta x} - \frac{u_i - u_{i-1}}{\Delta x}\right) \tag{1.2.3}$$

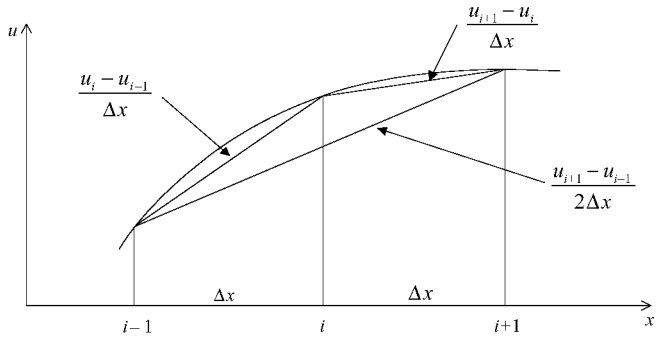

Figure 1.2.1 Finite difference approximations.

Substitute (1.2.3) into (1.2.1a) and use three grid points to obtain

$$\frac{u_{i+1} - 2u_i + u_{i-1}}{\Delta x^2} = 2 \tag{1.2.4}$$

With $u_{i-1} = 0$, $u_{i+1} = 0$, as specified by the given boundary conditions, the solution at $x = 1/2$ with $\Delta x = 1/2$ becomes $u_i = -1/4$. This is the same as the exact solution given by

$$u_i = (x^2 - x)_{x=\frac{1}{2}} = -\frac{1}{4} \tag{1.2.5}$$

In what follows, we shall demonstrate that the same exact solution is obtained, using other methods: FEM and FVM.

1.3 ONE-DIMENSIONAL COMPUTATIONS BY FINITE ELEMENT METHODS

For illustration, let us consider a one-dimensional domain as depicted in Figure 1.3.1a. Let the domain be divided into subdomains; say two local elements ($e = 1, 2$) in this example as shown in Figure 1.3.1b,c. The end points of elements are called nodes.

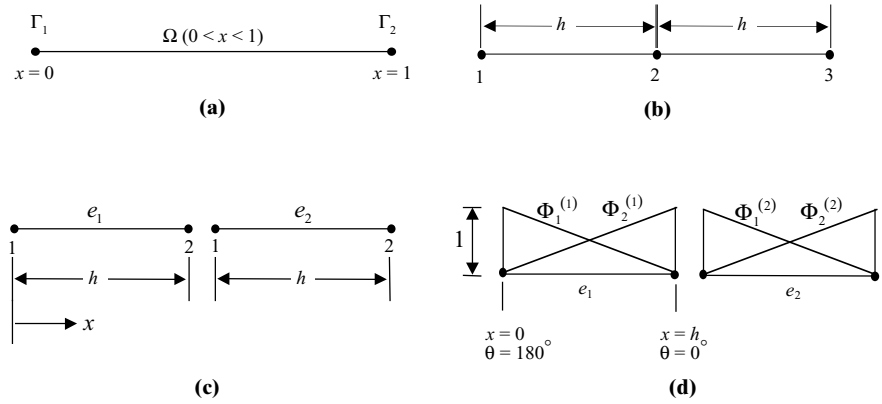

Figure 1.3.1 Finite element discretization for one-dimensional linear problem with two local elements. **(a)** Given domain (Ω) with boundaries ($\Gamma_1(x=0)$, $\Gamma_2(x=1)$). **(b)** Global nodes ($\alpha, \beta = 1, 2, 3$). **(c)** Local elements ($N, M = 1, 2$). **(d)** Local trial functions.

Assume that the variable $u^{(e)}(x)$ is a linear function of x

$$u^{(e)}(x) = \alpha_1 + \alpha_2 x \tag{1.3.1}$$

Write two equations from (1.3.1) for $x = 0$ (node 1) and for $x = h$ (node 2) in terms of the nodal values of variables, $u_1^{(e)}$ and $u_2^{(e)}$, solve for the constants α_1 and α_2, and substitute them back into (1.3.1). These steps lead to

$$u^{(e)}(x) = \left(1 - \frac{x}{h}\right)u_1^{(e)} + \left(\frac{x}{h}\right)u_2^{(e)} = \Phi_N^{(e)}(x)u_N^{(e)} \quad (N = 1, 2) \tag{1.3.2}$$

where the repeated index implies summing, $u_N^{(e)}$ represents the nodal value of u at the local node N for the element (e), and $\Phi_N^{(e)}(x)$ are called the local domain (element) *trial functions* (alternatively known as interpolation functions, shape functions, or basis functions),

$$\Phi_1^{(e)}(x) = 1 - \frac{x}{h}, \qquad \Phi_2^{(e)}(x) = \frac{x}{h} \tag{1.3.3a}$$

$$0 \le \Phi_N^{(e)}(x) \le 1 \tag{1.3.3b}$$

These functions are shown in Figure 1.3.1d, indicating that trial functions assume the value of one at the node under consideration and zero at the other node, linearly varying in between.

There are many different ways to formulate finite element equations (as detailed in Part Three). One of the simplest approaches is known as the Galerkin method. The basic idea is to construct an inner product of the residual $R^{(e)}$ of the local form of the governing equation (1.2.1a) with the *test functions* chosen the same as the trial functions given by (1.3.3) and in (1.3.2):

$$\left(\Phi_N^{(e)}(x),\, R^{(e)}\right) = \int_0^h \Phi_N^{(e)}(x)\left(\frac{d^2u^{(e)}(x)}{dx^2} - 2\right)dx = 0 \tag{1.3.4}$$

This represents an orthogonal projection of the residual error onto the subspace spanned by the test functions summed over the domain, which is then set equal to zero (implying that errors are minimized), leading to the best numerical approximation of the solution to the governing equation. Integrate (1.3.4) by parts to obtain

$$\overset{*}{\Phi}{}_N^{(e)}\frac{du}{dx}\bigg|_0^h - \int_0^h \frac{d\Phi_N^{(e)}(x)}{dx}\frac{du^{(e)}(x)}{dx}dx - \int_0^h 2\Phi_N^{(e)}(x)dx = 0$$

or by using (1.3.2), we have

$$\overset{*}{\Phi}{}_N^{(e)}\frac{du}{dx}\bigg|_0^h - \left[\int_0^h \frac{d\Phi_N^{(e)}(x)}{dx}\frac{d\Phi_M^{(e)}(x)}{dx}dx\right]u_M^{(e)} - \int_0^h 2\Phi_N^{(e)}(x)dx = 0 \quad (N, M = 1, 2) \tag{1.3.5}$$

This is known as the variational equation or *weak form* of the governing equation. Note that the second derivative in the given differential equation (1.2.1) has been transformed into a first derivative in (1.3.5), thus referred to as "weakened." This

implies that, instead of solving the second order differential equation directly, we are to solve the first order (weakened) integro-differential equation as given by (1.3.5), thus leading to a *weak solution*, as opposed to a *strong solution* that represents the analytical solution of (1.2.1). The derivative du/dx in the first term is no longer the variable within the domain, but it is the Neumann boundary condition (constant) to be specified at $x = 0$ or $x = h$ if so required. Likewise, the test function is no longer the function of x, thus given a special notation $\overset{*}{\Phi}{}_N^{(e)}$, called the Neumann boundary test function, as opposed to the domain test function $\Phi_N^{(e)}(x)$. The Neumann boundary test function assumes the value of 1 if the Neumann boundary condition is applied at node N, and 0 otherwise, similar to a Dirac delta function. This represents one of the limit values given by (1.3.3b) at $x = 0$ or $x = h$, indicating that it is no longer the function of x within the domain. Furthermore, appropriate direction cosines must be assigned, reduced from two-dimensional configurations (Figure 8.2.3). Depending on the Neumann boundary condition being applied on either the left-hand side ($x = 0$) or the right-hand side ($x = h$), we obtain

$$\left.\frac{du}{dx}\right|_{x=0} = \left.\frac{du}{dx}\cos\theta\right|_{\theta=180^\circ} = -\frac{du}{dx}, \qquad \left.\frac{du}{dx}\right|_{x=h} = \left.\frac{du}{dx}\cos\theta\right|_{\theta=0^\circ} = \frac{du}{dx} \tag{1.3.6a}$$

To prove (1.3.6a), we must first refer to the 2-D geometry as shown in Figure 8.2.3, and integration by parts is carried out as follows:

$$\iint \Phi_N^{(e)}(x)\frac{d^2u}{dx^2}dxdy \Rightarrow \int \overset{*}{\Phi}{}_N^{(e)}\frac{du}{dx}dy = \int \overset{*}{\Phi}{}_N^{(e)}\frac{du}{dx}\cos\theta\, d\Gamma = \overset{*}{\Phi}{}_N^{(e)}\frac{du}{dx}\cos\theta$$
$$= \overset{*}{\Phi}{}_N^{(e)}\frac{du}{dx}\Bigg|_{x=0,\theta=180^\circ}^{x=h,\theta=0^\circ} \tag{1.3.6b}$$

in which only the integrated term is shown (omitting the differentiated term) and the direction cosines for 1-D are applied at both ends of an element ($\theta = 0^\circ$ for $x = h$, $\theta = 180^\circ$ for $x = 0$). This represents the simplification of 2-D geometry into a 1-D problem.

Using a compact notation, we rewrite (1.3.5) as

$$K_{NM}^{(e)}\, u_M^{(e)} = F_N^{(e)} + G_N^{(e)} \quad (N, M = 1, 2) \tag{1.3.7}$$

This leads to a system of local algebraic finite element equations, consisting of the following quantities [henceforth the functional representation (x) in the domain trial and test functions will be omitted for simplicity unless confusion is likely to occur]:

Stiffness (Diffusion *or* Viscosity) Matrix (associated with the physics arising from the second derivative term)

$$K_{NM}^{(e)} = \int_0^h \frac{d\Phi_N^{(e)}}{dx}\frac{d\Phi_M^{(e)}}{dx}dx = \begin{bmatrix} \int_0^h \frac{d\Phi_1^{(e)}}{dx}\frac{d\Phi_1^{(e)}}{dx}dx & \int_0^h \frac{d\Phi_1^{(e)}}{dx}\frac{d\Phi_2^{(e)}}{dx}dx \\ \int_0^h \frac{d\Phi_2^{(e)}}{dx}\frac{d\Phi_1^{(e)}}{dx}dx & \int_0^h \frac{d\Phi_2^{(e)}}{dx}\frac{d\Phi_2^{(e)}}{dx}dx \end{bmatrix}$$
$$= \begin{bmatrix} K_{11}^{(e)} & K_{12}^{(e)} \\ K_{21}^{(e)} & K_{22}^{(e)} \end{bmatrix} = \frac{1}{h}\begin{bmatrix} 1 & -1 \\ -1 & 1 \end{bmatrix}$$

Source Vector

$$F_N^{(e)} = -\int_0^h 2\Phi_N^{(e)} dx = -h\begin{bmatrix}1\\1\end{bmatrix}$$

Neumann Boundary Vector

$$G_N^{(e)} = \overset{*}{\Phi}{}_N^{(e)} \frac{du}{dx}\bigg|_0^h = \overset{*}{\Phi}{}_N^{(e)} \frac{du}{dx}\cos\theta$$

Contributions of local elements calculated above ($e = 1, 2$) can be assembled into global nodes ($\alpha, \beta = 1, 2, 3$) simply by summing the adjacent elemental contributions to the global node shared by both elements. In this example, global node 2 is shared by local node 2 of element 1 and local node 1 of element 2.

$$K_{\alpha\beta} = \begin{bmatrix} K_{11} & K_{12} & K_{13} \\ K_{21} & K_{22} & K_{23} \\ K_{31} & K_{32} & K_{33} \end{bmatrix} = \begin{bmatrix} K_{11}^{(1)} & K_{12}^{(1)} & 0 \\ K_{21}^{(1)} & K_{22}^{(1)} + K_{11}^{(2)} & K_{12}^{(2)} \\ 0 & K_{21}^{(2)} & K_{22}^{(2)} \end{bmatrix} = \frac{1}{h}\begin{bmatrix} 1 & -1 & 0 \\ -1 & 2 & -1 \\ 0 & -1 & 1 \end{bmatrix} \tag{1.3.8}$$

$$F_\alpha = \begin{bmatrix} F_1 \\ F_2 \\ F_3 \end{bmatrix} = \begin{bmatrix} F_1^{(1)} \\ F_2^{(1)} + F_1^{(2)} \\ F_2^{(2)} \end{bmatrix} = -h\begin{bmatrix}1\\2\\1\end{bmatrix} \tag{1.3.9}$$

$$G_\alpha = \begin{bmatrix} G_1 \\ G_2 \\ G_3 \end{bmatrix} = \begin{bmatrix} G_1^{(1)} \\ G_2^{(1)} + G_1^{(2)} \\ G_2^{(2)} \end{bmatrix} = \begin{bmatrix} \overset{*}{\Phi}_1 \\ \overset{*}{\Phi}_2 \\ \overset{*}{\Phi}_3 \end{bmatrix} \frac{du}{dx}\cos\theta = \begin{bmatrix} \overset{*}{\Phi}{}_1^{(1)} \\ \overset{*}{\Phi}{}_2^{(1)} + \overset{*}{\Phi}{}_1^{(2)} \\ \overset{*}{\Phi}{}_2^{(2)} \end{bmatrix} \frac{du}{dx}\cos\theta$$

$$= \begin{bmatrix}0\\0\\0\end{bmatrix} \frac{du}{dx}\cos\theta \tag{1.3.10}$$

with $\overset{*}{\Phi}_1 = \overset{*}{\Phi}_2 = \overset{*}{\Phi}_3 = 0$ indicating that the Neumann boundary conditions are not to be applied to any of the global nodes for the solution of (1.2.1a,b). This implies that, if the Neumann boundary conditions are not applied, then the Neumann boundary vector is zero even if the gradient du/dx is not zero. If the Neumann boundary conditions are to be applied, then the boundary test function $\overset{*}{\Phi}_N^{(e)}$ assumes the value of one and the du/dx as given is simply imposed at the node under consideration. This is a part of the FEM formulation that makes the process more complicated than in FDM, but it is a distinct advantage when the Neumann boundary conditions are to be specified exactly.

Notice that the 2×2 local stiffness matrices for element 1 and element 2 are overlapped (superimposed) at the global node 2 with the contributions algebraically summed together,

$$K_{22} = K_{22}^{(1)} + K_{11}^{(2)}$$

and similarly,

$$F_2 = F_2^{(1)} + F_1^{(2)}, \qquad G_2 = G_2^{(1)} + G_1^{(2)}$$

In view of the above, we obtain the final global algebraic equations in the form

$$\begin{bmatrix} 1 & -1 & 0 \\ -1 & 2 & -1 \\ 0 & -1 & 1 \end{bmatrix} \begin{bmatrix} u_1 \\ u_2 \\ u_3 \end{bmatrix} = -h^2 \begin{bmatrix} 1 \\ 2 \\ 1 \end{bmatrix} \tag{1.3.11}$$

It will be shown in Chapter 8 that the global finite element equations (1.3.11) may be obtained directly from the global form of (1.3.4),

$$(\Phi_\alpha, R) = \int_0^1 \Phi_\alpha \left(\frac{d^2u}{dx^2} - 2 \right) dx = 0 \tag{1.3.12}$$

which will lead to (1.3.11), or

$$K_{\alpha\beta} u_\beta = F_\alpha + G_\alpha \quad (\alpha, \beta = 1, 2, 3) \tag{1.3.13}$$

Expanding (1.3.11) at the global node 2 yields

$$-u_1 + 2u_2 - u_3 = -2h^2 \quad (h = \Delta x) \tag{1.3.14}$$

or

$$\frac{u_{i+1} - 2u_i + u_{i-1}}{\Delta x^2} = 2 \tag{1.3.15}$$

This result is identical to the FDM formulation (1.2.4).

The Galerkin finite element method described here is called the standard Galerkin method (SGM). It works well for linear differential equations, but is not adequate for nonlinear problems in fluid mechanics. In this case, the test functions must be of the form different from the trial functions. This will be one of the topics to be discussed in Part Three.

1.4 ONE-DIMENSIONAL COMPUTATIONS BY FINITE VOLUME METHODS

Finite volume methods (FVM) utilize the control volumes and control surfaces as depicted in Figure 1.4.1. The control volume for node i covers $\Delta x/2$ to the right and left of node i with the control surface being located at $i - 1/2$ and $i + 1/2$. Finite volume formulations can be obtained either by a finite difference basis or a finite element basis. The results are identical for one-dimensional problems.

1.4.1 FVM VIA FDM

The basic idea for the formulation of FVM is similar to the finite element method (1.3.12) with the test function being set equal to unity, as applied to the differential equation (1.2.1a),

$$(\Phi_\alpha, R) = (1, R) = \int_0^1 (1) \left(\frac{d^2u}{dx^2} - 2 \right) dx = 0, \quad 0 < x < 1 \tag{1.4.1}$$

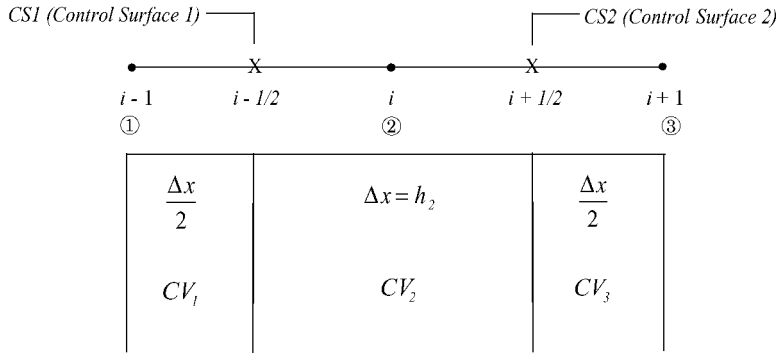

Figure 1.4.1 Finite volume approximations.

Integrating (1.4.1) yields

$$\left.\frac{du}{dx}\right|_0^1 - \int_0^1 2dx = 0 \tag{1.4.2a}$$

or

$$\sum_{CS1,2} \frac{\Delta u}{\Delta x} - \sum_{CV2} 2\Delta x = 0 \tag{1.4.2b}$$

The integration limits of 0 and 1 are now replaced by discrete control surfaces ($CS1$ and $CS2$) between $i - 1/2$ and $i + 1/2$, and the source term is to be evaluated for the control volume ($CV2$), with reference to Figure 1.4.1. This implies that du/dx in (1.4.2a) is to be evaluated at the control surfaces and that the diffusion flux du/dx is conserved between $i - 1$ and i through the control surface $i - 1/2$ or $CS1$ and between i and $i + 1$ through the control surface $i + 1/2$ or $CS2$. This is accomplished when the control surface equations are assembled at $i - 1, i$, and $i + 1$. This conservation property is the most significant aspect of the finite volume methods.

To complete the illustrative process, (1.4.2) can be written using finite difference representation for the control surfaces between $i - 1/2$ and $i + 1/2$ as

$$\underset{(CS2)}{\frac{u_{i+1} - u_i}{\Delta x}} - \underset{(CS1)}{\frac{u_i - u_{i-1}}{\Delta x}} = \underset{(CV2)}{2\Delta x} \tag{1.4.3}$$

Dividing (1.4.3) by Δx, we obtain

$$\frac{u_{i+1} - 2u_i + u_{i-1}}{\Delta x^2} = 2 \tag{1.4.4}$$

which is identical to (1.2.4) for the finite difference method. Note that $CV1$ and $CV3$ do not contribute to this process since nodes $i - 1$ and $i + 1$ are the boundaries whose influence is contained in (1.4.3) through control surfaces $CS1$ and $CS2$.

1.4.2 FVM VIA FEM

In order to demonstrate that FVM can also be formulated by FEM, we evaluate du/dx analytically from the trial functions (1.3.2), (Figure 1.3.1d), for the finite volume representation of (1.4.2a),

$$u^{(e)} = \Phi_N^{(e)} u_N^{(e)} = \left(1 - \frac{x}{h}\right) u_1^{(e)} + \frac{x}{h} u_2^{(e)}$$

or

$$\frac{du^{(e)}}{dx} = \frac{u_2^{(e)} - u_1^{(e)}}{h}$$

so that, from (1.3.6), we obtain

$$\left.\frac{du^{(1)}}{dx}\right|_{CS1} = \left.\frac{u_2^{(1)} - u_1^{(1)}}{h} \cos\theta\right|_{\theta=180^\circ} = \frac{u_2^{(1)} - u_1^{(1)}}{h}(-1) \tag{1.4.5}$$

$$\left.\frac{du^{(2)}}{dx}\right|_{CS2} = \left.\frac{u_2^{(2)} - u_1^{(2)}}{h} \cos\theta\right|_{\theta=0^\circ} = \frac{u_2^{(2)} - u_1^{(2)}}{h}(1) \tag{1.4.6}$$

Here, $CS1$ provides the direction cosine, $\cos\theta = \cos 180^\circ = -1$, whereas $CS2$ gives $\cos\theta = \cos 0^\circ = 1$, with reference to Figure 1.4.1.

Summing the fluxes through $CS1$ and $CS2$ at the control volume center (node 2) in terms of the global nodes

$$\sum_{CS1,2} \frac{du}{dx} = \frac{u_2 - u_1}{h}(-1) + \frac{u_3 - u_2}{h}(1) \tag{1.4.7}$$

Note that, using (1.4.7), the finite volume representation (1.4.2) is given by

$$\frac{u_3 - 2u_2 + u_1}{\Delta x^2} = 2 \tag{1.4.8}$$

Once again, the result is the same as all other previous analyses.

1.5 NEUMANN BOUNDARY CONDITIONS

So far, we have dealt with only the Dirichlet boundary conditions for numerical examples. However, it has been seen that the Neumann boundary condition, du/dx, arises automatically from the finite element or finite volume formulations through integration by parts. This information, if given as an input, may be implemented at the boundary nodes under consideration. This is not the case for finite difference methods.

To demonstrate this point, let us return to the differential equation examined in Section 1.2.

$$\frac{d^2u}{dx^2} - 2 = 0 \quad 0 < x < 1 \tag{1.5.1}$$

with the following boundary conditions:

$$u(0) = 0 \qquad \text{(Dirichlet)} \quad \text{at } x = 0 \tag{1.5.2}$$

$$\frac{du}{dx}(1) = 1 \qquad \text{(Neumann)} \quad \text{at } x = 1 \tag{1.5.3}$$

where it is reminded that the given differential equation (1.5.1) is described only within the domain, $0 < x < 1$, not including the boundaries, $x = 0$ and $x = 1$, which are reserved for the specification of boundary conditions, either Dirichlet or Neumann. Only when the governing equation is integrated are the boundary points ($x = 0, x = 1$) needed and used.

In the following subsections, implementations of the Neumann boundary conditions will be demonstrated.

1.5.1 FDM

One way to implement the Neumann boundary condition of the type (1.5.3) is to install a phantom (ghost, imaginary, fictitious) node 4 as shown in Figure 1.5.1. Writing the finite difference equation and the Neumann boundary condition (slope) at the boundary node 3, we have

$$u_4 - 2u_3 + u_2 = 2\Delta x^2 \tag{1.5.4}$$

$$\frac{u_4 - u_2}{2\Delta x} = 1 \tag{1.5.5}$$

Substitute (1.5.5) into (1.5.4),

$$2\Delta x + u_2 - 2u_3 + u_2 = 2\Delta x^2 \tag{1.5.6}$$

Writing the finite difference equation at node 2, we have

$$u_3 - 2u_2 + u_1 = 2\Delta x^2 \tag{1.5.7}$$

Solve (1.5.6) and (1.5.7) simultaneously to obtain

$$u_2 = -1/4, \quad \text{with } u_3 = 0$$

which is the exact solution. This is because the approximation given by (1.5.5) is reasonable with respect to the exact solution. The phantom node method may give a large

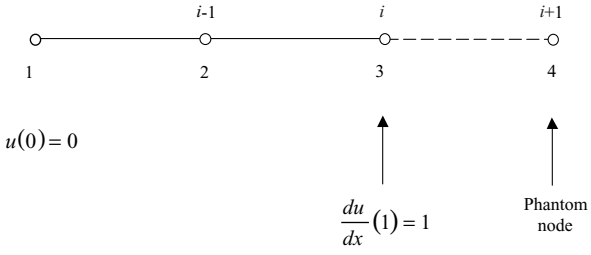

Figure 1.5.1 Installation of phantom node for Neumann boundary condition in finite difference method.

error if this is not the case, or if the solution is unsymmetric with respect to the interior and phantom node.

Instead of using a phantom node, we may utilize the higher order finite difference equation at the Neumann boundary node. For example, we use the second order accurate finite difference formula for du/dx at node 3 (see Chapter 3 for derivation),

$$\left(\frac{du}{dx}\right)_3 = \frac{3u_3 - 4u_2 + u_1}{2\Delta x} = 1 \tag{1.5.8}$$

Solve u_3 from the above and substitute the result into (1.5.7) and obtain once again the exact solution $u_2 = -1/4, u_3 = 0$.

1.5.2 FEM

It follows from (1.3.6b) that, at the Neumann boundary node 3,

$$G_N^{(e)} = \overset{*}{\Phi}{}_N^{(e)} \frac{du}{dx}\bigg|_0^h, \quad with\ \overset{*}{\Phi}{}_3^{(e)} = 1 \tag{1.5.9a}$$

Thus

$$G_3 = (1)\frac{du}{dx}\bigg|_{x=h} = (1)\frac{du}{dx}\cos 0^\circ = 1 \tag{1.5.9b}$$

It follows from (1.3.11) that, having applied the Dirichlet boundary condition at node 1 ($u(0) = 0$), the global finite element equation becomes

$$\begin{bmatrix} 2 & -1 \\ -1 & 1 \end{bmatrix} \begin{bmatrix} u_2 \\ u_3 \end{bmatrix} = -h^2 \begin{bmatrix} 2 \\ 1 \end{bmatrix} + h \begin{bmatrix} 0 \\ 1 \end{bmatrix} \tag{1.5.10}$$

from which we obtain the exact solution $u_2 = -1/4$ and $u_3 = 0$. Notice that FEM accommodates the Neumann boundary conditions exactly within the formulation itself, not through those approximations required in FDM.

At this point it is important to realize that, if the Neumann boundary condition $du/dx = -1$ is specified on the left end, then we have

$$G_1 = \frac{du}{dx}\bigg|_{x=0} = \frac{du}{dx}\cos 180^\circ = (-1)(-1) = 1$$

Thus, we have

$$\begin{bmatrix} 1 & -1 \\ -1 & 2 \end{bmatrix} \begin{bmatrix} u_1 \\ u_2 \end{bmatrix} = -h^2 \begin{bmatrix} 1 \\ 2 \end{bmatrix} + h \begin{bmatrix} 1 \\ 0 \end{bmatrix}$$

This will once again give the exact solution, $u_1 = 0$ and $u_2 = -1/4$.

1.5.3 FVM VIA FDM

The finite volume equation is given by Figure 1.4.1,

$$\frac{du}{dx}\bigg|_{i-\frac{1}{2}}^{i+\frac{1}{2}} - \int_{i-\frac{1}{2}}^{i+\frac{1}{2}} 2dx = 0$$

or in terms of finite differences at node 2,

$$\frac{u_3 - u_2}{\Delta x} - \frac{u_2 - u_1}{\Delta x} - 2\Delta x = 0 \tag{1.5.11}$$

at node 3,

$$\left.\frac{du}{dx}\right|_3 - \left.\frac{du}{dx}\right|_{i+\frac{1}{2}} - 2\frac{\Delta x}{2} = 0 \quad \text{or} \quad 1 - \frac{u_3 - u_2}{\Delta x} - 2\frac{\Delta x}{2} = 0 \tag{1.5.12}$$

Combining (1.5.11) and (1.5.12), we obtain

$$\begin{bmatrix} 2 & -1 \\ -1 & 1 \end{bmatrix} \begin{bmatrix} u_2 \\ u_3 \end{bmatrix} = -h^2 \begin{bmatrix} 2 \\ 1 \end{bmatrix} + h \begin{bmatrix} 0 \\ 1 \end{bmatrix}$$

It is interesting to note that this is identical to the FEM formulation (1.5.10). Solving, we have the exact solution ($u_2 = -1/4, u_3 = 0$). In this manner, FVM via FDM is capable of implementing the Neumann boundary conditions exactly, unlike FDM.

1.5.4 FVM VIA FEM

We return to (1.4.2a),

$$\left.\frac{du}{dx}\right|_0^1 - \int_0^1 2dx = 0 \tag{1.5.13}$$

where at node 2 we have, from (1.4.5) and (1.4.6),

$$\left.\frac{du}{dx}\right|_0^1 - \int_0^1 2dx = \frac{du}{dx}\cos 180^\circ + \frac{du}{dx}\cos 0^\circ - 2h$$

or

$$\frac{u_2 - u_1}{h}(-1) + \frac{u_3 - u_2}{h}(1) - 2h = 0 \tag{1.5.14}$$

at node 3,

$$\left.\frac{du}{dx}\right|_{2\frac{1}{2}} + \left.\frac{du}{dx}\right|_3 - 2\frac{h}{2} = 0$$

or

$$\frac{u_3 - u_2}{h}(-1) + 1 - h = 0 \tag{1.5.15}$$

Combining (1.5.14) and (1.5.15), we have

$$\begin{bmatrix} 2 & -1 \\ -1 & 1 \end{bmatrix} \begin{bmatrix} u_2 \\ u_3 \end{bmatrix} = \begin{bmatrix} -2h^2 \\ h - h^2 \end{bmatrix}$$

This gives the exact solution, $u_2 = -1/4$ and $u_3 = 0$. Once again in FVM via FEM the treatment of the Neumann boundary condition is precise.

1.6 EXAMPLE PROBLEMS

Here we provide additional examples, illustrating further applications of boundary conditions and including treatment of source terms.

1.6.1 DIRICHLET BOUNDARY CONDITIONS

Consider the three-element system as shown in Figure 1.6.1a to solve the differential equation with the source term $f(x)$,

$$\frac{d^2u}{dx^2} - 2u = f(x) \quad 0 < x < 1 \tag{1.6.1}$$
$$f(x) = 4x^2 - 2x - 4$$

subject to the Dirichlet boundary conditions:

$$u = 0 \quad \text{at } x = 0$$
$$u = -1 \quad \text{at } x = 1$$

whose exact solution is given by $u = -2x^2 + x$.

FDM

Write FDE at nodes 2 and 3.

Node 2

$$\frac{u_3 - 2u_2 + u_1}{\Delta x^2} - 2u_2 = f_2$$
$$\frac{u_3 - 2u_2 + 0}{(1/3)^2} - 2u_2 = 4\left(\frac{1}{3}\right)^2 - 2\left(\frac{1}{3}\right) - 4 = \frac{-38}{9}$$
$$9(u_3 - 2u_2) - 2u_2 = \frac{-38}{9}$$

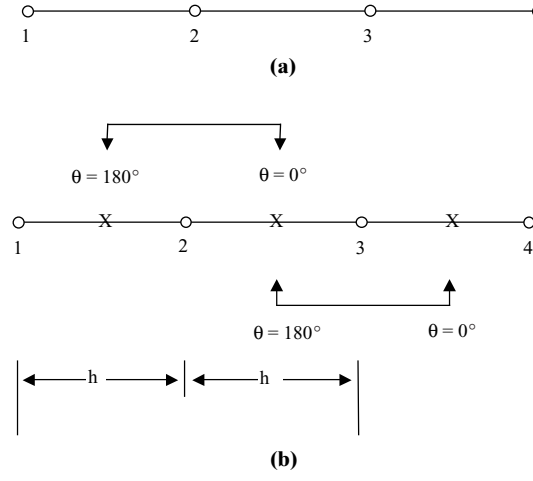

Figure 1.6.1 Example problem, Dirichlet and Neumann boundary conditions. **(a)** Three elements, four nodes for FDM and FEM. **(b)** Direction cosines at control surfaces as a result of integration by parts for FVM.

Node 3

$$\frac{u_4 - 2u_3 + u_2}{(1/3)^2} - 2u_3 = 4\left(\frac{2}{3}\right)^2 - 2\left(\frac{2}{3}\right) - 4 = \frac{-32}{9}$$

$$9(-1 - 2u_3 + u_2) - 2u_3 = \frac{-32}{9}$$

Combining, we have

$$\begin{bmatrix} -20 & 9 \\ 9 & -20 \end{bmatrix} \begin{bmatrix} u_2 \\ u_3 \end{bmatrix} = \begin{bmatrix} -\frac{38}{9} \\ \frac{49}{9} \end{bmatrix}$$

$$\begin{bmatrix} u_2 \\ u_3 \end{bmatrix} = \begin{bmatrix} 0.111 \\ -0.222 \end{bmatrix}$$

These values represent the exact solution.

FEM

The local Galerkin finite element analog is given by

$$\int_0^h \Phi_N^{(e)} \left(\frac{d^2u}{dx^2} - 2u - f(x) \right) dx = 0$$

where the source term $f(x)$ may be linearly approximated in the form

$$f(x) = \Phi_N^{(e)}(x) f_N^{(e)}$$

Integrating by part, the local algebraic equations are written as

$$K_{NM}^{(e)} u_M^{(e)} = F_N^{(e)} + G_N^{(e)}$$

where

$$K_{NM}^{(e)} = \int_0^h \left(\frac{d\Phi_N^{(e)}}{dx} \frac{d\Phi_M^{(e)}}{dx} + 2\Phi_N^{(e)} \Phi_M^{(e)} \right) dx = \frac{1}{h} \begin{bmatrix} 1 & -1 \\ -1 & 1 \end{bmatrix} + \frac{2h}{6} \begin{bmatrix} 2 & 1 \\ 1 & 2 \end{bmatrix}$$

$$F_N^{(e)} = C_{NM}^{(e)} f_M^{(e)}, \qquad C_{NM}^{(e)} = -\int_0^h \Phi_N^{(e)} \Phi_M^{(e)} dx = -\frac{h}{6} \begin{bmatrix} 2 & 1 \\ 1 & 2 \end{bmatrix}, \qquad G_{NM}^{(e)} = \begin{bmatrix} 0 \\ 0 \end{bmatrix}$$

The local finite element equations are assembled into the global form,

$$K_{\alpha\beta} u_\beta = F_\alpha + G_\alpha$$

or

$$\begin{bmatrix} a & b & 0 & 0 \\ b & c & b & 0 \\ 0 & b & c & b \\ 0 & 0 & b & a \end{bmatrix} \begin{bmatrix} u_1 \\ u_2 \\ u_3 \\ u_4 \end{bmatrix} = -\frac{h}{6} \begin{bmatrix} 2 & 1 & 0 & 0 \\ 1 & 4 & 1 & 0 \\ 0 & 1 & 4 & 1 \\ 0 & 0 & 1 & 2 \end{bmatrix} \begin{bmatrix} f_1 \\ f_2 \\ f_3 \\ f_4 \end{bmatrix} + \frac{du}{dx} \begin{bmatrix} 0 \\ 0 \\ 0 \\ 0 \end{bmatrix}$$

$$= -\frac{h}{6} \begin{bmatrix} 2f_1 + f_2 \\ f_1 + 4f_2 + f_3 \\ f_2 + 4f_3 + f_4 \\ f_3 + 2f_4 \end{bmatrix} = \frac{h}{54} \begin{bmatrix} 110 \\ 220 \\ 184 \\ 68 \end{bmatrix}$$

with

$$a = (1/h) + (2h/3) = 29/9$$
$$b = -(1/h) + (2h/6) = -26/9,$$
$$c = 58/9$$

$$f_\beta = \begin{bmatrix} f_1 \\ f_2 \\ f_3 \\ f_4 \end{bmatrix} = \begin{bmatrix} -4 \\ -\frac{38}{9} \\ -\frac{32}{9} \\ -2 \end{bmatrix}$$

The first and last equations are replaced by the Dirichlet boundary conditions $u(0) = 0$ and $u(1) = -1$, and the rest of the equations are modified as follows:

$$u_1 = 0$$
$$cu_2 + bu_3 = F_2$$
$$bu_2 + cu_3 + b\,(-1) = F_3$$
$$u_4 = -1$$

Rewriting the above in matrix form,

$$\begin{bmatrix} 1 & 0 & 0 & 0 \\ 0 & c & b & 0 \\ 0 & b & c & 0 \\ 0 & 0 & 0 & 1 \end{bmatrix} \begin{bmatrix} u_1 \\ u_2 \\ u_3 \\ u_4 \end{bmatrix} = \begin{bmatrix} 0 \\ F_2 \\ F_3 \\ -1 \end{bmatrix} - \begin{bmatrix} 0 \\ 0 \\ -b \\ 0 \end{bmatrix}$$

The solution of the above equations again results in the exact solution,

$$\begin{bmatrix} u_1 \\ u_2 \\ u_3 \\ u_4 \end{bmatrix} = \begin{bmatrix} 0 \\ 0.111 \\ -0.222 \\ -1 \end{bmatrix}$$

Notice that the first and last equations may be deleted and only the second and third equations solved to once again arrive at the exact solution.

FVM via FDM

Finite volume methods require the use of control volumes and control surfaces centered around a node. The governing differential equation is integrated similarly as in finite element formulations, but with the test functions set equal to unity at a node under consideration and zero elsewhere. At node 2 for control volume 1, we have

$$\int_{x_i - \frac{1}{2} = 1\frac{1}{2}}^{x_i + \frac{1}{2} = 2\frac{1}{2}} (1)\left[\frac{d^2u}{dx^2} - 2u - f(x)\right]dx = 0$$

$$\frac{du}{dx}\Big|_{1\frac{1}{2}}^{2\frac{1}{2}} - \int_{1\frac{1}{2}}^{2\frac{1}{2}} 2u dx = \int_{1\frac{1}{2}}^{2\frac{1}{2}} f(x)dx, \qquad \frac{u_3 - u_2}{\Delta x} - \frac{u_2 - u_1}{\Delta x} - 2u_2\Delta x = f_2\Delta x$$

Similarly, at node 3 for control volume 2

$$\frac{u_4 - u_3}{\Delta x} - \frac{u_3 - u_2}{\Delta x} - 2u_3\Delta x = f_3\Delta x$$

These equations are identical to FDM, giving the exact solution.

FVM via FEM

$$\left.\frac{du}{dx}\right|_0^1 - \int_0^1 2u dx = \int_0^1 f(x)dx$$

For control volume 1 with *CS*1 and *CS*2 involved, we have

$$\sum_{CS1,2} \frac{du}{dx} = \frac{u_2 - u_1}{h}(\cos 180^\circ) + \frac{u_3 - u_2}{h}(\cos 0^\circ) = \frac{u_2 - u_1}{h}(-1) + \frac{u_3 - u_2}{h} \quad (1)$$

$$\frac{u_3 - 2u_2 + u_1}{h} - 2u_2 h = f_2 h$$

or

$$\frac{u_3 - 2u_2 + u_1}{\Delta x^2} - 2u_2 = f_2$$

Similarly, for control volume 2 with *CS*1 and *CS*2 involved,

$$\frac{u_4 - 2u_3 + u_2}{\Delta x^2} - 2u_3 = f_3$$

It is seen that the result is identical to FVM via FDM.

1.6.2 NEUMANN BOUNDARY CONDITIONS

Here we demonstrate methods for treating the Neumann boundary conditions depending on the side of the boundary to which they are applied.

Neumann Boundary Condition Specified at Right End Node. Given the same differential equation as in (1.6.1), Figure 1.6.1b:

$$\frac{d^2u}{dx^2} - 2u = f(x) \quad 0 < x < 1$$

$$f(x) = 4x^2 - 2x - 4$$

subject to boundary conditions:

$$u = 0 \qquad \text{at } x = 0$$

$$\frac{du}{dx} = -3 \quad \text{at } x = 1$$

which has the exact solution:

$$u = -2x^2 + x$$

FDM

From the given Neumann boundary conditions without using the phantom node, we have

$$\frac{u_4 - u_3}{(1/3)} = -3, \qquad u_4 = u_3 - 1$$

with FDM equations at nodes 2 and 3 given by

$$\frac{u_3 - 2u_2 + u_1}{(1/3)^2} - 2u_2 = f_2$$

$$\frac{u_4 - 2u_3 + u_2}{(1/3)^2} - 2u_3 = f_3$$

Thus we obtain

$$9(u_3 - 2u_2 + 0) - 2u_2 = -\frac{38}{9}$$

$$9(u_3 - 1 - 2u_3 + u_2) - 2u_3 = -\frac{32}{9}$$

or

$$\begin{bmatrix} -20 & 9 \\ 9 & -11 \end{bmatrix} \begin{bmatrix} u_2 \\ u_3 \end{bmatrix} = \begin{bmatrix} -\frac{38}{9} \\ -\frac{32}{9} \end{bmatrix} + \begin{bmatrix} 0 \\ 9 \end{bmatrix} = \begin{bmatrix} -\frac{38}{9} \\ \frac{49}{9} \end{bmatrix}$$

or

$$\begin{bmatrix} u_2 \\ u_3 \end{bmatrix} = \begin{bmatrix} -0.018 \\ -0.51 \end{bmatrix}$$

$$u_4 = -1 - 0.51 = -1.51, \quad 50\% \text{ error}$$

In order to improve the solution, we may use a three-element system with the phantom node 5,

$$\left.\frac{du}{dx}\right|_{x=1} = -3 = \frac{u_5 - u_3}{2\Delta x}, \qquad u_5 = u_3 - 2$$

$$9u_3 - 20u_4 + 9u_5 = f_4$$

$$9u_3 - 20u_4 + 9(u_3 - 2) = -2$$

$$\begin{bmatrix} -20 & 9 & 0 \\ 9 & -20 & 9 \\ 0 & 18 & -20 \end{bmatrix} \begin{bmatrix} u_2 \\ u_3 \\ u_4 \end{bmatrix} = \begin{bmatrix} -\frac{38}{9} \\ -\frac{32}{9} \\ 16 \end{bmatrix}$$

This gives the exact solution

$$u_1 = 0, \qquad u_2 = 1/9, \qquad u_3 = -2/9, \qquad u_4 = -1$$

Another method is to use the second order accurate formula for du/dx [(3.2.5) or (3.2.20) in Chapter 3] written at node 4,

$$\frac{3u_4 - 4u_3 + u_2}{2\Delta x} = -3$$

or with d^2u/dx^2 written at node 4 as

$$\frac{\left(\frac{du}{dx}\right)_4 - \left(\frac{du}{dx}\right)_{4-\frac{1}{2}}}{\Delta x/2} = \frac{2}{\Delta x}\left(-3 - \frac{u_4 - u_3}{\Delta x}\right)$$

and combining with FDM equations written at nodes 2 and 3, we again obtain the exact solution. The reader may verify that the solution deteriorates significantly if only two elements are used. This is because the implementation of Neumann boundary conditions is difficult in FDM, contrary to FEM, as shown in the next example.

FEM

The Neumann boundary conditions at $x = 1$ are written as

$$G_N^{(e)} = \overset{*}{\Phi}_N \frac{du}{dx}\bigg|_0^h, \qquad G_2^{(2)} = (1)\left(\frac{du}{dx}\right)_2 = -3$$

with $\overset{*}{\Phi}_N = 0$ everywhere except at the Neumann boundary node. Assembly of all contributions of elements for the global stiffness matrix and the load vector for a two-element system results in the following:

$$\begin{bmatrix} c & b \\ b & a \end{bmatrix}\begin{bmatrix} u_2 \\ u_3 \end{bmatrix} = \frac{-h}{6}\begin{bmatrix} f_1 + 4f_2 + f_3 \\ f_2 + 2f_3 \end{bmatrix} = -\frac{1}{12}\begin{bmatrix} -22 \\ -8 \end{bmatrix}$$

with

$$a = (1/h) + (2h/3) = 2 + 1/3 = 7/3$$
$$b = -(1/h) + (h/3) = -2 + 1/6 = -11/6$$
$$c = 14/3$$

so that the final algebraic equations together with the Neumann boundary vector are written as

$$\begin{bmatrix} \frac{14}{3} & -\frac{11}{6} \\ -\frac{11}{6} & \frac{7}{3} \end{bmatrix}\begin{bmatrix} u_2 \\ u_3 \end{bmatrix} = \frac{1}{12}\begin{bmatrix} 22 \\ 8 \end{bmatrix} + \begin{bmatrix} 0 \\ -3 \end{bmatrix}$$

or

$$\begin{bmatrix} u_2 \\ u_3 \end{bmatrix} = \begin{bmatrix} 0 \\ -1 \end{bmatrix}$$

Once again, the exact solution has been obtained with only two elements.

FVM via FEM and FDM (two elements)

For node 3 via FEM, we have

$$\frac{du}{dx}\bigg|_{2\frac{1}{2}} + \frac{du}{dx}\bigg|_3 - 2u_3\frac{h}{2} = f_3\frac{h}{2}$$
$$\frac{u_3 - u_2}{h}(-1) - 3 - 2u_3\frac{h}{2} = -2\left(\frac{h}{2}\right)$$

Similarly, for node 3 via FDM, we obtain

$$\left.\frac{du}{dx}\right|_{2\frac{1}{2}}^{3} - 2u_3\frac{h}{2} = f_3\frac{h}{2}$$

$$-3 - \frac{u_3 - u_2}{h} - 2u_3\frac{h}{2} = -2\left(\frac{h}{2}\right)$$

Thus, for both methods, we have

$$\begin{bmatrix} -\frac{5}{2} & 1 \\ 1 & -\frac{5}{4} \end{bmatrix}\begin{bmatrix} u_2 \\ u_3 \end{bmatrix} = \begin{bmatrix} -1 \\ \frac{5}{4} \end{bmatrix}$$

or

$$\begin{bmatrix} u_2 \\ u_3 \end{bmatrix} = \begin{bmatrix} 0 \\ -1 \end{bmatrix}$$

It is seen that both methods give the same results.

Neumann Boundary Condition Specified at Left End Node. To demonstrate treatment of the Neumann boundary condition if given at the left end node, we consider the following data:

$$\frac{du}{dx} = 1 \quad at\ x = 0$$
$$u = -1 \quad at\ x = 1$$

FDM

(1) Phantom node method (phantom node created, corresponding to u_0)

$$\frac{u_2 - u_0}{2\Delta x} = 1$$

(2) Second order accurate formula for du/dx at node 1

$$\frac{-3u_1 + 4u_2 - u_3}{2\Delta x} = 1$$

(3) d^2u/dx^2 written at node 1 as

$$-\frac{\left(\frac{du}{dx}\right)_1 - \left(\frac{du}{dx}\right)_{1\frac{1}{2}}}{\frac{\Delta x}{2}} = \frac{-2}{\Delta x}\left(1 - \frac{u_2 - u_1}{\Delta x}\right)$$

With either one of these three methods, we obtain the exact solution. The reader should carry out the calculations for verification of the above results.

FEM

$$\begin{bmatrix} a & b & 0 \\ b & c & b \\ 0 & b & a \end{bmatrix}\begin{bmatrix} u_1 \\ u_2 \\ u_3 \end{bmatrix} = \begin{bmatrix} F_1 \\ F_2 \\ F_3 \end{bmatrix} + \begin{bmatrix} \overset{*}{\Phi}_1 \left.\frac{du}{dx}\right|_{x=0} \\ 0 \\ 0 \end{bmatrix}$$

with

$$\overset{*}{\Phi}_1 \left.\frac{du}{dx}\right|_{x=0} = (1)\frac{du}{dx}\cos(180^\circ) = (1)(1)(-1)$$

$$\begin{bmatrix} 2.333 & -1.888 & 0 \\ -1.888 & 4.666 & -1.833 \\ 0 & -1.833 & 2.333 \end{bmatrix} \begin{bmatrix} u_1 \\ u_2 \\ u_3 \end{bmatrix} = \begin{bmatrix} 1 \\ 1.833 \\ 0.666 \end{bmatrix} + \begin{bmatrix} -1 \\ 0 \\ 0 \end{bmatrix}$$

$$\begin{bmatrix} u_1 \\ u_2 \\ u_3 \end{bmatrix} = \begin{bmatrix} 0 \\ 0 \\ -1 \end{bmatrix}$$

Note that, although $\frac{du}{dx}(0) = 1$ at the left end node, we obtain $G_1 = -1$ because of the direction cosine, $\cos 180^\circ = -1$. The reader is reminded that it is important to recognize the role of direction cosines as depicted in Figure 8.2.3.

FVM via FEM

$$\text{Node 1:} \quad \left.\frac{du}{dx}\right|_1 + \left.\frac{du}{dx}\right|_{1\frac{1}{2}} - 2u_1\frac{h}{2} = f_1\frac{h}{2}$$

$$\text{Node 2:} \quad \left.\frac{du}{dx}\right|_{1\frac{1}{2}} + \left.\frac{du}{dx}\right|_{2\frac{1}{2}} - 2u_2 h = f_2 h$$

Specifying the Neumann boundary data with correct direction cosine (-1), we obtain

$$\text{Node 1:} \quad (1)(-1) + \frac{u_2 - u_1}{h}(1) - 2u_1\left(\frac{h}{2}\right) = -4\left(\frac{h}{2}\right)$$

$$\text{Node 2:} \quad \frac{u_2 - u_1}{h}(-1) + \frac{u_3 - u_2}{h}(1) - 2u_2 h = -4h$$

$$\begin{bmatrix} -\frac{5}{4} & 1 \\ 1 & -\frac{5}{2} \end{bmatrix} \begin{bmatrix} u_1 \\ u_2 \end{bmatrix} = \begin{bmatrix} 0 \\ 0 \end{bmatrix}$$

from which, again, we obtain the same results.

FVM via FDM

$$\text{Node 1:} \quad \left.\frac{du}{dx}\right|_1^{1\frac{1}{2}} = \frac{u_2 - u_1}{h} - 1$$

$$\text{Node 2:} \quad \left.\frac{du}{dx}\right|_{1\frac{1}{2}}^{2\frac{1}{2}} = \frac{u_3 - u_2}{h} - \frac{u_2 - u_1}{h}$$

The formulation and results here are the same as in FVM via FEM.

1.7 SUMMARY

The purpose of this chapter was to acquaint the reader with all available computational methods through very simple one-dimensional linear second order differential

equations. For one-dimensional problems presented in this chapter, it is seen that all methods, finite differences, finite elements, and finite volumes provide the final forms of algebraic equations identical to each other, giving the same results for Dirichlet problems. Neumann boundary conditions are approximated in FDM, but they are implemented exactly in FEM and FVM. They "naturally" arise in due course of the formulation. For this reason, Neumann boundary condition is often called "natural" boundary condition. This is not the case for FDM, although exact solutions were obtained for simple examples.

The formulation of FDM equations in one dimension is simple, whereas the concept of algebra involved in FEM is complex. This complicated algebra, however, will be quite useful in multidimensional, arbitrary geometries, and boundary conditions.

Although we have shown only one-dimensional problems in this chapter, we may be able to predict what will happen in multidimensional problems. Mesh configurations for FDM must be *structured* for multidimensional problems as shown in Figure 1.7.1a. Inclined or curved mesh lines can be transformed into orthogonal coordinates so that finite difference equations can be written in orthogonal directions for 2-D or 3-D. This can not be done for FDM if the mesh configuration is *unstructured* as in Figure 1.7.1b. In this case, FEM and FVM can still be accommodated to arbitrary geometries and arbitrary mesh configurations (triangular or quadrilateral elements for 2-D, tetrahedral or hexahedral elements for 3-D).

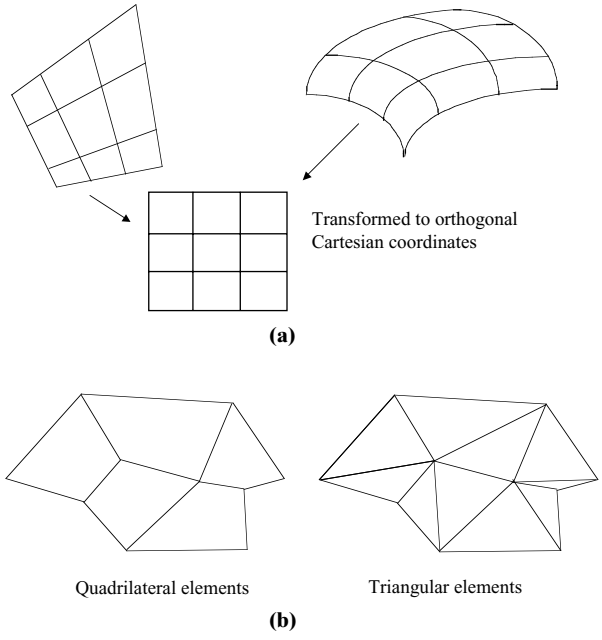

Figure 1.7.1 Geometric mesh configurations in two dimensions. **(a)** Structured grids for finite difference, mesh lines intersecting two ways (2-D) and three ways (3-D). They must be transformed into orthogonal cartesian coordinates. **(b)** Unstructured grids for finite elements or finite volumes. No coordinate transformations are required.

There are differences and analogies (similarities) among all methods, irrespective of geometric dimensions. Some of the relatively well known properties are listed below.

FDM

1. Easy to formulate.
2. For multidimensional problems, meshes must be structured in either two or three dimensions. Curved meshes must be transformed into orthogonal cartesian coordinates so that finite difference equations can be written on structured cartesian meshes.
3. Neumann boundary conditions can only be approximated, not exactly enforced.

FEM

1. Underlying principles and formulations require a mathematical rigor.
2. Complex geometries and unstructured meshes are easily accommodated, no coordinate transformations needed.
3. Neumann boundary conditions are enforced exactly.

FVM

1. Formulations can be based on either FDM or FEM.
2. Surface integrals of normal fluxes guarantee the conservation properties throughout the domain.
3. Complex geometries and unstructured meshes are easily accommodated, no coordinate transformations needed.

The above assessments are by no means complete; we shall examine more thoroughly all the details of each method in the remainder of this book. Advantages and disadvantages are to be evaluated on a much broader basis.

Many of the problems in fluids and heat transfer are dominated by convection, shock wave discontinuities, turbulence microscales, incompressibility, compressibility, viscosity, etc. Thus the simple procedures shown in this chapter must be modified in accordance with physical situations. These challenges are ahead of us. Our goal is to explore all major computational methods using FDM, FEM, and FVM in the hope that in the end the reader will have developed an insight and ability to choose the most accurate, efficient, and suitable approaches to CFD in order to solve his or her problems of interest.

REFERENCES

Anderson, J. D., Jr. [1995]. *Computational Fluid Dynamics*. New York: McGraw-Hill.

Anderson, D. A., Tannehill, J. C., and Pletcher, R. H. [1984]. *Computational Fluid Mechanics and Heat Transfer*. New York: McGraw-Hill.

Baker, A. J. [1983]. *Finite Element Computational Fluid Mechanics*. New York: Hemisphere, McGraw-Hill.

Beam, R. M. and Warming, R. F. [1978]. An implicit factored scheme for the compressible Navier-Stokes equations. *AIAA J.*, 16, 393–401.

Briley, W. R. and McDonald, H. [1973]. Solution of the Three-dimensional Compressible Navier-Stokes Equations by an Impucit Technique. Proc. Fourth Int. Conf. Num. Methods Fluid

Dyn., Boulder, Colorado. *Lecture Notes in Physics*. Vol. 35. New York: Springer-Verlag, pp. 105–110.
Carey, G. and Oden, J. T. [1986]. *Finite Elements, Fluid Mechanics*. Vol. 6. Englewood Cliffs, NJ: Prentice Hall.
Chung, T. J. [1978]. *Finite Element Analysis in Fluid Dynamics,* McGraw-Hill.
———. [1999]. Transitions and interactions of inviscid/viscous, compressible/incompressible and laminar/turbulent flows. *Int. J. Num. Methods in Fluids,* 31, 223–46.
Courant, R., Friedrichs, K. O., and Lewy, H. [1928]. Uber die partiellen differenz-gleichungen der mathematischen Physik. *Mathematische Annalen*, 100, 32–74. *IBM J*. [1967], 215–34. [English translation].
Donea, J. [1984]. A Taylor-Galerkin method for convective transport problems. *Int. J. Num. Methods Eng.*, 20, 101–19.
Evans, M. E. and Harlow, F. H. [1957]. The Particle-in-Cell Method for Hydrodynamic Calculations, Los Alamos Scientific Laboratory Report LA-2139. Los Alamos: New Mexico.
Ferziger, J. H. and Peric, M. [1999]. *Computational Methods for Fluid Dynamics*. Berlin: Springer-Verlag.
Fletcher, C. A. [1988]. *Computational Techniques for Fluid Dynamics*. Vol. 1: Fundamental and General Techniques. Berlin: Springer-Verlag.
———. [1988]. *Computational Techniques for Fluid Dynamics*. Vol. 2: Specific Techniques for Different Flow Categories. Berlin: Springer-Verlag.
Godunov, S. K. [1959]. A difference scheme for numerical computation of discontinuous solutions of hydrodynamic equations (in Russian). *Math. Sibornik*, 47, 271–306. United States Joint Publications Research Service, JPRS 7226 [1960]. [English translation].
Gresho, P. M. and Sani, R. L. [1999]. *Incompressible Flows and Finite Element Method*. New York: Wiley.
Harten, A. [1978]. The artificial compression method for computation of shocks and contact discontinuities. III. Self-adjusting hybrid schemes. *Math. Comput*, 32, 363–89.
———. [1983]. High resolution schemes for hyperbolic conservation laws. *J. Comp. Physics*, 49, 357–93.
Heinrich, J. C., Huyakorn, P. S., Zienkiewicz, O. C., and Mitchell, A. R. [1977]. An upwind finite element scheme for two-dimensional convective transport equation. *Int. J. Num. Meth. Eng.*, 11, no. 1, 131–44.
Hirsch, C. [1988]. *Numerical Computation of Internal and External Flows*, Vol. 1: Fundamentals of Numerical Discretization, New York: Wiley.
———. [1990]. *Numerical Computation of Internal and External Flows*, Vol. 2: Computational Methods for Inviscid and Viscous Flows, New York: Wiley.
Hoffmann, K. A. [1989]. *Computational Fluid Dynamics for Engineers*, Engineering Education System, Austin, TX.
Hughes, T. J. R. and Brooks, A. N. [1982]. A theoretical framework for Petrov-Galerkin methods with discontinuous weighting functions: application to the streamline upwind procedure. In R. H. Gallagher, et al. (eds). *Finite Elements in Fluids*, London: Wiley.
Hughes, T., and Mallet, M. [1986]. A new finite element formulation for computational fluid dynamics: IV. A discontinuity capturing operator for multidimensional advective-diffusive systems. *Comp. Meth. Appl. Mech. Eng.*, 58, 329–36.
Hughes, T., Franca, L., and Mallet, M. [1986]. A new finite element formulation for computational fluid dynamics: I. Symmetric forms of the compressible Euler and Navier-Stokes equations and the second law of thermodynamics. *Comp. Meth. Appl. Mech. Eng.*, 54, 223–34.
Hughes, T., Mallet, M., and Mizukami, A. [1986]. A new finite element formulation for computational fluid dynamics: It. Beyond SUPG, *Comp. Meth. Appl. Mech. Eng.*, 54, 341–55.
Jameson, A. [1982]. Transonic aerofoil calculations using the Euler equations. In P. L. Roe (ed.) *Numerical Methods in Aeronautical Fluid Dynamics*, New York: Academic Press.

Johnson, C. [1987]. *Numerical Solution of Partial Differential Equation's on the Finite Element Method*, Lund, Sweden: Student Litteratur.

Lax, P. D. and Wendroff, B. [1960]. Systems of conservation laws. *Comm. Pure and Appl. Math.*, 13, 217–37.

Löhner, R., Morgan, K., and Zienkiewicz, O. C. [1985]. An adaptive finite element procedure for compressible high speed flows. *Comp. Meth. Appl. Mech. Eng.*, 51, 441–65.

MacCormack, R. W. [1969]. The effect of viscosity in hypervelocity impact cratering. AIAA Paper 69–354, Cincinnati, Ohio.

Oden, J. T. [1972]. *Finite Elements of Non Linear Continua*. New York: McGraw-Hill.

———. [1988]. *Adaptive FEM in Complex Flow Problems. The Mathematics of Finite Elements with Applications*. Edited by J. R. Whiteman, London Academic Press, Vol. 6, 1–29.

Oden, J. T., Babuska, I., and Baumann, C. E. [1998]. A discontinuous *hp* finite element method for diffusion problems. *J. Comp. Phys.*, 146, 491–519.

Oden, J. T. and Demkowicz, L. [1991]. h-p adaptive finite element methods in computational fluid dynamics. *Comp. Meth. Appl. Mech. Eng.*, 89 (1–3): 1140.

Oden, J. T., Demkowicz, L., Rachowicz, W., and Westerman, T. A. [1989]. Toward a universal *h-p* adaptive finite element strategy, Part 2: A posteriori error estimation, *Comp. Meth. Appl. Mech. Eng.* 77, 113–80.

Oden, J. T. and Wellford, L. C. Jr. [1972]. Analysis of viscous flow by the finite element method. *AIAA J*, 10, 1590–9.

Patankar, S. V. [1980]. *Numerical Heat Transfer and Fluid Flow*. New York: Hemisphere/McGraw-Hill.

Pepper, D. W. and Heinrich, J. [1992]. *The Finite Element Method: Basic Concepts and Applications*. UK: Taylor & Francis.

Peyret, R. and Taylor, T. D. [1983]. *Computational Methods for Fluid Flow*. New York: Springer-Verlag.

Pironneaau, O. [1989]. *Finite Element Methods for Flows*. New York: Wiley.

Richardson, L. F. [1910]. The approximate arithmetical solution by finite differences of physical problems involving differential equations with an application to the stresses in masonry dam. *Trans. Roy. Soc. Lond.*, Ser. A, 210, 307–57.

Roe, P. L. [1981]. Approximate Riemann solvers, parameter vectors and difference schemes. *J. Comp. Phys.*, 43, 357–72.

———. [1984]. Generalized formulation of TVD Lax-Wendroff schemes. ICASE Report 84-53. NASA CR-172478, NASA Langley Research Center.

Roache, P. J. [1972]. *Computational Fluid Dynamics*, Albuquerque, NM: Hermosa Publications.

———. [1999]. *Fundamentals of Computational Fluid Dynamics*. Albuquerque, NM: Hermosa Publications.

Tannehill, J. C., Anderson, D. A., and Pletcher, R. H. [1997]. *Computational Fluid Mechanics and Heat Transfer*. 2nd ed., New York: McGraw-Hill.

Turner, M. J., Clough, R. W., Martin, H. C., and Topp, L. P. [1956]. Stiffness and deflection analysis of complex structures. *J. Aeron. Soc.*, 23, 805–23.

Van Leer, B. [1974]. Towards the ultimate conservative difference scheme. II. Monotonicity and conservation combined in a second order scheme. *J. Comp. Phys.*, 14, 361–70.

Zienkiewicz, O. C. and Cheung, Y. K. [1965]. Finite elements in the solution of field problems. *The Engineer*, 507–10.

Zienkiewicz, O. C., and Codina, R. [1995]. A general algorithm for compressible and incompressible flow – Part I. Characteristic-based scheme. *Int. J. Num. Methods in Fluids*, 20, 869–85.

Zienkiewicz, O. C., and Taylor, R. L. [1991]. The *Finite Element Method*, Vol. 2. New York: McGraw-Hill.